

ATMOSPHERIC RESPONSE AND FEEDBACK TO SMOKE  
RADIATIVE FORCING FROM WILDLAND FIRESYongqiang Liu  
USDA Forest Service, Athens, Georgia**1. INTRODUCTION**

Smoke from wildland fires is one of the sources of atmospheric anthropogenic aerosols. It can dramatically affect regional and global radiative balance. Ross et al. (1998) estimated a direct radiative forcing of nearly  $-20 \text{ Wm}^{-2}$  for the 1995 Amazonian smoke season (August and September). Penner et al. (1992) indicated that the magnitude of the smoke global radiative forcing is comparable to that of anthropogenic aerosols.

Aerosol radiative forcing can result in changes in regional atmospheric dynamics, clouds and precipitation. These changes, on the other hand, could feedback aerosol radiative forcing by, for example, modifying total incoming solar radiation, a mechanism known as semi-direct aerosol radiative forcing (Hanson et al., 1997). Atmospheric feedback has been recognized as an extremely important factor for the magnitude of the greenhouse gas effects (Washington, 1992).

This study investigates regional atmospheric response and feedback to smoke direct radiative forcing from extensive wildland fires using a dynamical model and a regional climate model.

**2. MODELS AND SIMULATIONS****2.1 Analytical Model**

An atmospheric dynamical model with smoke aerosol radiative forcing is constructed to obtain analytical evidence for atmospheric response to large-scale smoke aerosol radiative forcing and the associated physical processes. The model consists of a set of zonally symmetric equations for hydrostatic, nondivergent, and zonally geostrophic perturbation motions. The equation set is the same as the one used by Charney (1975) for the bio-geophysical self-feedback mechanism except the inclusion of vertical eddy heat transfer and aerosol radiative forcing.

Radiative forcing of the Earth-atmosphere system due to aerosols is calculated by a scheme proposed by Charlson et al. (1992). The radiative effects of smoke aerosols are taken into account in two ways, the absorption of solar radiation by aerosols, which directly heats the atmosphere, and the change in the surface radiative balance as a low boundary condition of the model. The model parameters are specified based on the Smoke, Clouds and Radiation-Brazil (SCAR-B) experiments (Kauffman et al., 1998).

**2.2 Three-Dimensional Model**

The National Center for Atmospheric Research (NCAR) Regional Climate Model (RegCM, Dickinson et al., 1989; Giorgi and Bates, 1989) is used to simulate atmospheric response, including changes in clouds and precipitation. RegCM was developed to study regional features of climate and land-surface processes by incorporating improved schemes of a number of critically important climate processes into the NCAR/Penn State Mesoscale Model (MM4/5). The model calculates radiative effects of aerosols using the NCAR column radiative model (CRM, Kiehl and Briegleb, 1993) and the land-atmospheric exchanges using the Biosphere-Atmosphere Transfer Scheme (BATS, Dickinson et al., 1993).

The simulation domain is centered at  $15^{\circ}\text{S}$ ,  $57.5^{\circ}\text{W}$ , and contains  $91 \times 91$  grid points with a spacing of 60 km and 14 vertical layers. RegCM is integrated for August and September of 1995, when the SCAR-B was conducted. The atmospheric initial and horizontal lateral boundary conditions are interpolated from the analysis of the European Center for Medium Range Weather Forecast (ECMWF). The sea-surface temperature (SST) in the adjacent oceans is specified from a set of monthly means (Shea et al. 1992).

A control run of smoke-free case and an experiment run with smoke loading during the SCAR-B period are performed with RegCM. In the experiment run, the optical depth, single scattering albedo (SSA) and asymmetric factor of smoke in the experiment are specified based on the SCAR-B measurements. The midvisible optical depth of 0.75 is adopted (Ross et al., 1998). An SSA of 0.88 is specified for absorption smoke, based on the measured range of 0.82-0.94 at approximately 550 nm (Eck et al., 1998). The wavelength dependencies of the optical properties are determined mainly based on the fourth-order polynomials (Ross et al., 1998). Humidification effect has been included in the optical depth. Geographically,

---

•Corresponding author address: Yongqiang Liu, Forest Sciences Laboratory, 320 Green Street, Athens, GA 30602; e-mail: [yliu@fs.fed.us](mailto:yliu@fs.fed.us)

the optical depth is the same over the smoke region in the northern South America (approximately the area of less than  $-10 \text{ Wm}^{-2}$  in Figure 2a). The optical depth of 0.14 is assumed for the mountains and oceans, and 0.28 for rest of the continental. The vertical extent of the smoke is assumed the lowest 3 km.

The smoke direct radiative forcing (DRF) with atmospheric feedback is measured by the difference in the net solar radiation flux at the top of the model atmosphere between the RegCM experiment and control runs, and the atmospheric response by the differences in various atmospheric variables. The DRF without atmospheric feedback is estimated by conducting off-line simulations with CRM. CRM is run at individual RegCM grids with fixed air temperature, air humidity, cloud fraction, and cloud water path specified using the RegCM control-run outputs at four times (i.e., 0, 6, 12, and 18 GMT) averaged over the simulation period.

### 3. RESULTS

#### 3.1 Dynamics of Atmospheric Response

The solutions of the dynamical model represent a horizontally symmetric two layer structure of a strong cool, descending layer in the lower troposphere and a weak warm, ascending one in the middle and upper troposphere (Figure 1).

Temperature perturbation is determined by the relative importance of two mechanisms with opposite contributions. The eddy transfer of the surface sensible heat flux, which is reduced because of the negative radiative forcing of smoke, leads to decreased temperature, while aerosol absorption of solar radiation leads to increased temperature. The magnitude of the former is greater below about 3 km and, therefore, the temperature perturbation is negative. It is opposite above that height.

Experiments are conducted to examine variations of the perturbations on the surface with a number of factors. The magnitudes of both the temperature and velocity perturbations increase with smoke optical depth and decrease with cloud fraction. They increase with both SSA and Bowen ratio, which are proportional to the heat transfer. The magnitude of the temperature perturbation increases with the size of smoke region while that of the velocity perturbation, which is proportional to second-order derivation of horizontal distance, varies oppositely. The perturbation in vertical motion is more significant in lower latitudes and in an anticyclonic circulation background due to a weak effect of the Earth rotation. The height of the interface of the two different layers varies significantly with SSA, from about 1 km for an SSA of 0.5 to the top of the atmosphere for an SSA of 1.

#### 3.2 Direct Radiative Forcing

The smoke DRF simulated with CRM ranges from  $-10$  to  $-20 \text{ Wm}^{-2}$  over the smoke region (Figure 2a). Its magnitude is larger in the eastern Amazonia where cloud water path is smaller than the western Amazonia (Figure 3a), comparable to the DRF of  $-15 \pm 5 \text{ Wm}^{-2}$  for a tropical location within the biomass burning region in Brazil obtained by Ross et al. (1998). The smoke DRF simulated with RegCM displays a similar spatial pattern, but its magnitude is much smaller, especially in the southwestern portion of the smoke region (Figure 2b).

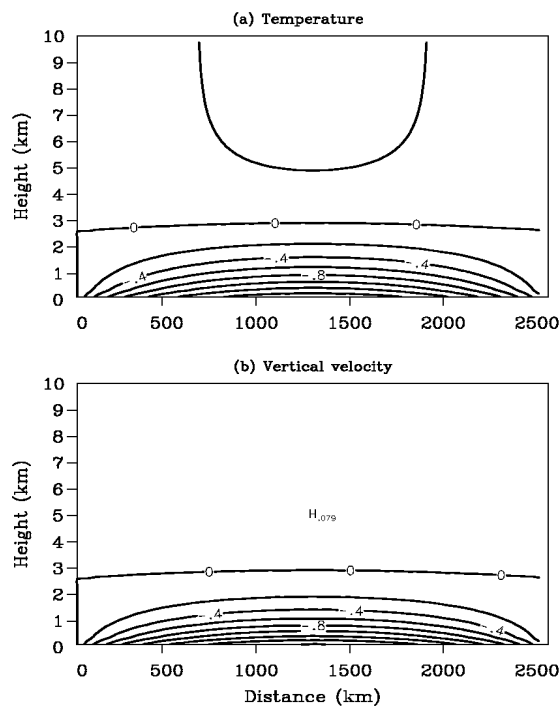


Figure 1 Perturbations in temperature ( $^{\circ}\text{C}$ ) and vertical velocity ( $10^{-3} \text{ ms}^{-1}$ ).

#### 3.3 Changes in Clouds and Feedback

The larger reduction in the DRF magnitude apparently corresponds to the significant reduction in clouds in the same areas (Figure 3b), suggesting that feedback from the cloud changes should be a major contributor to the DRF reduction. An additional evidence for the important role of cloud changes can be obtained from the difference in DRF between clear- and cloudy-sky atmosphere. The smoke-region averaged DRF simulated with CRM is about  $-17$  and  $-15 \text{ Wm}^{-2}$  for clear and cloudy sky, respectively. The magnitude is reduced for cloudy sky because the amount of total solar radiation itself, to which the magnitude of the smoke DRF is proportional, becomes smaller in a cloudy sky because clouds reflect some solar radiation. The corresponding values for RegCM are  $-16$  and  $-8 \text{ Wm}^{-2}$ , showing a much larger reduction in the magnitude for cloudy sky. This is attributed to

the reduced clouds due to the smoke radiative forcing in addition to the cloud-reflection effect. The cloud reduction allows more incoming solar radiation, which in turn leads to opposite changes to the smoke DRF: it reduces the magnitude of the smoke DRF by directly compensating the loss of the solar radiation due to the smoke, and increases the magnitude due to the cloud-reflection effect (but with an opposite direction). The overwhelming reduced smoke DRF suggests that the first process should be a dominant mechanism.

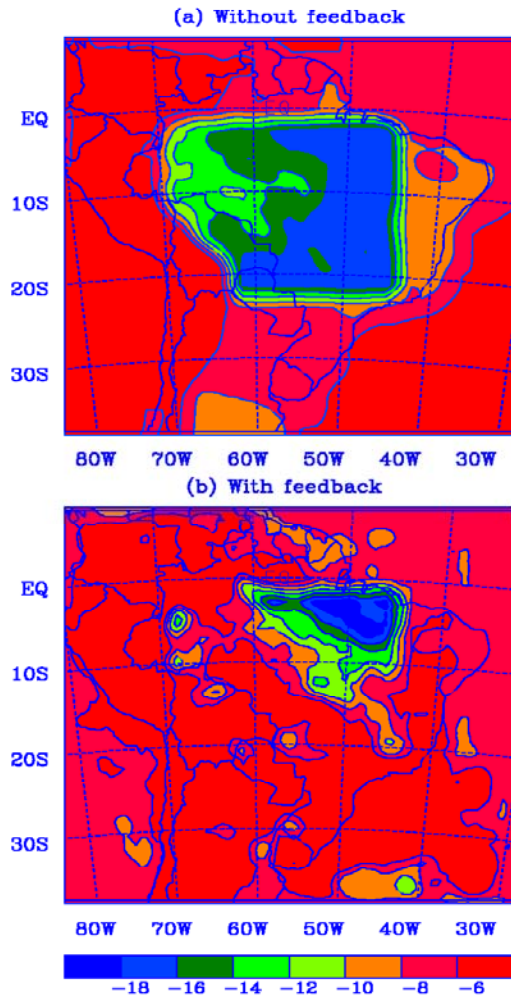


Figure 2 Direct radiative forcing of wildland fire smoke during August and September, 1995 ( $Wm^{-2}$ ) without (a) and with (b) atmospheric feedback.

The cloud reduction is resulted from the perturbations in atmospheric dynamics and the associated water vapor transport. The surface sensible heat flux simulated with RegCM is reduced by  $42 Wm^{-2}$ , about half of its original magnitude, due to a reduction by  $51 Wm^{-2}$  in the surface solar radiation. This leads to cooling and subsidence motion in the air above the surface with the temperature perturbation of about  $-2^{\circ}C$  on the surface (Figure 4). The transfer of water vapor from PBL to the cloud layer becomes

smaller due to the combined effects of weaker turbulent activities and the resistance from the subsidence tendency. As a result, more water vapor is retained in PBL instead of transferred to the cloud layer. Relative humidity is reduced by about 15%. Clouds are reduced in response to the reduction in relative humidity, which is a primary factor for the dominant non-convective precipitation during the smoke season in Amazonia. Note that the increase in the temperature at the cloud levels also contributes to the negative perturbation of relative humidity but it has a very limited role. This is different from the "cloud burning" over the Indian Ocean (Ackerman et al., 2000), in which relative humidity's reduction is caused by warming due to aerosol absorption of solar radiation.

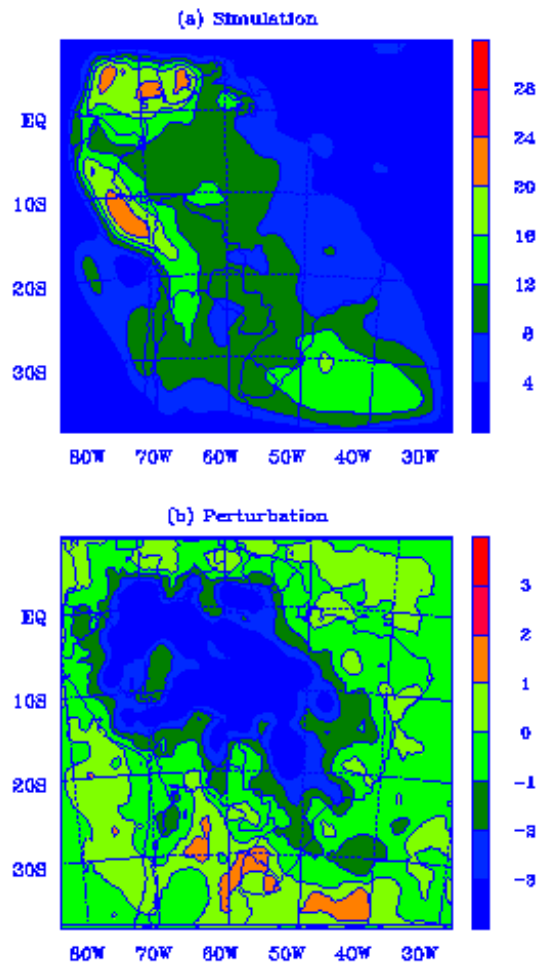


Figure 3 Simulation (a) and perturbation (b) of cloud water path ( $gm^{-2}$ ) simulated with RegCM.

A weak warm layer with ascending motion above 2 km is formed, which is resulted from the absorption of solar radiation by the smoke. To examine the role of the absorption, two additional experiment runs are performed with the SSA values of 0.82 and 0.94,

representing young (strong absorption) and aged smoke (light absorption), respectively. The smoke with light absorption produces stronger subsidence tendency, which almost offsets the original ascending motion within 2 km. In contrast, the smoke with strong absorption produces a deep ascending layer above the planetary-boundary layer (PBL).

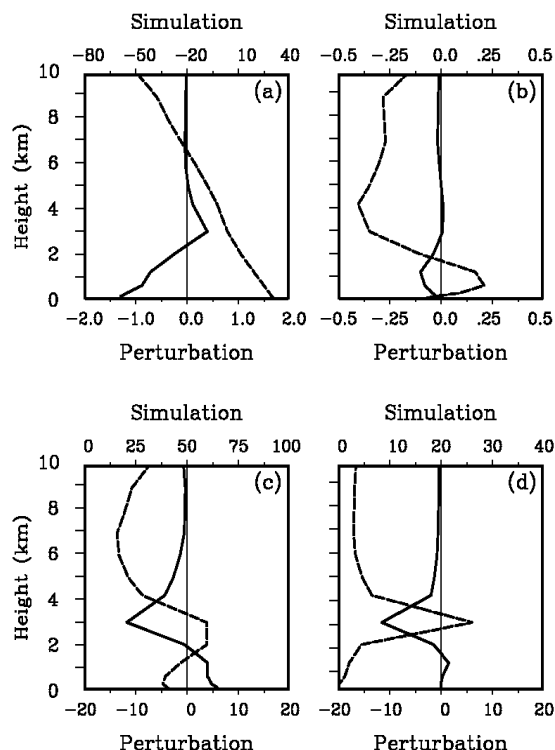


Figure 4 Vertical profiles of atmospheric variables averaged over the smoke region simulated with RegCM. Panels (a)-(d) are temperature ( $^{\circ}\text{C}$ ), vertical velocity ( $10^{-3}\text{m/s}$ ), relative humidity (%), and cloud water path ( $\text{gm}^{-2}$ ). The solid and dashed lines represent atmospheric response and the control run.

#### 4. Concluding Remarks

The dynamical analyses and numerical simulations have indicated a structure of a cooler subsidence layer topped by a warmer ascending one in the atmospheric response to large-scale smoke. The upper layer seems similar to the radiative-convective layer in the oil-fire smoke dynamics (Herring and Hobbs 1994). However, the ascending rate here is much smaller and, more importantly, it is accompanied by a strong cool and descending layer below.

Clouds are reduced in response to the reduction in relative humidity. Different from the "cloud burning" mechanism (Ackerman et al. 2000), in which relative humidity reduction is caused by warming due to aerosol

absorption of solar radiation, weaker turbulent activity due to reduced surface sensible heat flux and resistance from the perturbed PBL subsidence reduce transfer of water vapor from PBL to cloud layer.

The direct radiative forcing of large-scale smoke from biomass burning is reduced substantially due to the feedback of the reduction in clouds. The feedback is more significant in the western Amazonia, where more clouds exist during the dry season, than in the eastern Amazonia. The atmospheric perturbations induced by the large-scale smoke may contribute to the formation of the vertical dual peaks of optical depth (Ross et al. 1998). The ascending motions in the warmer layer generated by smoke with strong absorption can transport aerosol particles to the height of about 3 km or higher in certain circumstance.

The ascending motion in the atmospheric dynamical perturbations due to the smoke DRF can lift some smoke particles from PBL to a higher elevation to form another smoke layer in addition to the one in PBL. There were observed dual peaks of optical depth, one near the surface and the other at about 3 km, in some SCAR-B measurements (Ross et al., 1998). Also, over one-third of vertical profiles observed during the Indian Ocean Experiment (INDOEX) had elevated layers of aerosols with strong absorption, decoupled from the surface (Andravs et al., 2001). The warm and ascending layer seems similar to the radiative-convective layer in the oil-fire smoke dynamics (Herring and Hobbs, 1994) except that the upward motion is much slower and accompanied by a cool, downward motion below.

The atmospheric perturbations due to the large-scale smoke may suggest the presence of a so-called self-contained mechanism of smoke particles with light absorption, similar to the bio-geophysical mechanism in the desert dynamics proposed by Charley (1975). The smoke particles lead to negative radiative forcing; The atmosphere responds by generating a descending tendency in PBL; This tends to retain more smoke particles in PBL, which leads to larger magnitude of radiative forcing.

#### References

Ackerman, A.S., O.B. Toon, D.E. Stevens, A.J. Heymsfield, V. Ramanathan, E.J. Welton, 2000: Reduction of tropical cloudiness by soot. *Science*, **288**, 1042-1047.

Andravs, E., D. Jackson, A. Jefferson, J. Ogren, P. Sheridan, and J. Wendell, 2001: Aerosols and radiation. In *Climate Monitoring and Diagnostics Laboratory Summer Report*, No. 25 (1998-1999) (Eds. D. Delene (for the paper), R.C. Schnell, D.B. King, and R.M. Rosson (for the Report)).

- Charlson, R.J., S.E. Schwartz, J.M. Hales, R.D. Cess, J.A. Coakley Jr., J.E. Hansen and D.J. Hoffman, 1992: Climate forcing by anthropogenic sulfate aerosols. *Science*, **255**, 423-430.
- Charney, J.B., 1975: Dynamics of deserts and drought in the Sahel. *Q.J.Roy. Meteor. Soc.*, **101**, 193-202.
- Dickinson, R. E., R. M. Errico, F. Giorgi, and G. T., Bates, 1989: A regional climate model for the western U.S. *J. Climate*, **15**, 383-422.
- Dickinson, R. E., A. Henderson-Seller, P.J. Kennedy, and F. Giorgi, 1993: *Biosphere-Atmosphere Transfer Scheme (BATS) version 1e as Coupled to the NCAR Community Climate Model*. Tech. Note, NCAR/TN, National Center for Atmospheric Research, Boulder, CO.
- Eck T.F., B.N. Holben, I. Slutsker, and A. Setzer, 1998: Measurements of irradiance attenuation and estimation of aerosol single scattering albedo for biomass burning aerosols in Amazonia. *J. Geophys. Res.*, **103**, 31865-31878.
- Giorgi, F. and G. T. Bates, 1989: The climatological skill of a regional model over complex terrain. *Mon. Wea. Rev.*, **117**, 2325-2347.
- Hansen J., M.Sato, and R. Ruedy, 1997: Radiative forcing and climate response. *J. Geophys. Res.*, **102**, 6831-6864.
- Herring J.A. and P.V. Hobbs, 1994: Radiatively driven dynamics of the plume from 1991 Kuwait oil fires. *J. Geophys. Res.*, **99**, 18809-18826.
- Hobbs, P.V., J.S. Reid, R.A. Kotchenruther, R.J. Ferek, and R. Weiss, 1997: Direct radiative forcing by smoke from biomass burning. *Science*, **275**, 1176-1178.
- Kauffman Y.J., P.V. Hobbs, V.W.J.H. Kirchhoff, P. Artaxo, L.A. Remer, B.N. Holben, M.D. King, D.E. Ward, E.M. Prins, K.M. Longo, L.F. Mattos, C.A. Nobre, J.D. Spinhirne, Q. Ji, A.M. Thompson, J.F. Gleason, S.A., Christopher, and S.-C. Tsay, 1998: Smoke, Clouds, and Radiation-Brazil (SCAR-B) experiment. *J. Geophys. Res.*, **103**, 31783-31808.
- Kiehl, J.T., and B.P. Briegleb, 1993: The relative role of sulfate aerosols and greenhouse gases in climate forcing, *Science*, **260**, 311-314.
- Penner, J.E., R.E. Dickinson, and C.S. O'Neill, 1992: Effects of aerosol from biomass burning on the global radiation budget. *Science*, **256**, 1432-1434.
- Ross J.L., P.V. Hobbs and B. Holben, 1998: Radiative characteristics of regional hazes dominated by smoke from biomass burning in Brazil: Closure tests and direct radiative forcing. *J. Geophys. Res.*, **103**, 31925-31941.
- Shea, D.J., K.E. Trenberth, and R.W. Reynolds, 1992: A global monthly sea surface temperature climatology. *J. Clim.*, **5**, 987-1001.
- Washington, W.M., 1992: Climate-model response to increased CO<sub>2</sub> and other greenhouse gases. In *Climate System Modeling* (ed. K.E. Trenberth), Cambridge Uni. Press, 643-668.